Irreversible saturation transitions in dimer-dimer reaction models of heterogeneous catalysis

1992 J. Phys. A: Math. Gen. 25 2557

(http://iopscience.iop.org/0305-4470/25/9/026)

J. Phys. A: Math. Gen. **25** (1992) 2557-2568. Printed in the UK

Irreversible saturation transitions in dimer–dimer reaction models of heterogeneous catalysis

Ezequiel V Albano

Instituto de Investigaciones Fisicoquímicas Teóricas y Aplicadas, (INIFTA), Facultad de Ciencias Exactas, Universidad Nacional de La Plata, Casilla de Correo 16, Suc 4 (1900), La Plata, Argentina

Received 19 August 1991, in final form 5 January 1992

Abstract. The dynamics and the critical behaviour of dimer-dimer surface reactions of the type $\frac{1}{2}A_2 + B_2 \rightarrow B_2A$ are investigated by means of Monte Carlo simulations and finite-size analysis. Three models, which follow the Langmuir-Hinshelwood mechanism and involves the formation of intermediate AB-species are proposed and studied. Neglecting both diffusion and desorption of the reactants (model M1), a critical point (p_{1B_2}) is found at $p_{1B_2} = \frac{2}{3}$ (p_{B_2} is the partial pressure of B_2-dimers in the gas phase), such that for $p_{B_2} < \frac{2}{3}$ ($p_{B_2} > \frac{2}{3}$) the surface becomes irreversibly saturated by a 'binary compound' of A and AB-species (B-species), respectively. The reaction proceeds only at $p_B = \frac{2}{3}$. Assuming B-diffusion (model M2) the critical point remains unchanged and the main features of M2 are basically the same as those of M1. The third model (M3) considers the recombination reaction of adsorbed B-species leading to a dimer desorption. M3 has a critical point at $p_{1B_2} \simeq 0.7014$, as it follows from a finite-size analysis. For $p_{B_2} \leqslant p_{1B_2}$ the surface is saturated by A and AB-species, while for $p_{B_2} > p_{1B_2}$ a reaction window with B_2A production is found. So, at p_{1B_2} one has an irreversible transition from an off-equilibrium saturated state to a stationary regime with sustained reaction. The critical behaviour of the rate of production and the reactant's coverage is analysed and the corresponding critical exponents are evaluated.

1. Introduction

Very recently there has been considerable interest in the study of microscopic models based upon the Langmuir-Hinshelwood mechanism for heterogeneously catalysed reactions [1-21]. The simplest case is the irreversible monomer-monomer (MM) reaction scheme of the type $A + B \rightarrow AB$, which has a critical point at $p_B = \frac{1}{2}$ (p_B is the partial pressure of B-monomers in the gas phase) [2, 4, 6, 13, 14]. Assuming finite desorption probabilities for both reactants, the MM scheme exhibits a rich variety of dynamical phenomena such as self-sustained oscillations, bistability and chaos [7, 8].

A more complex model is the irreversible dimer-monomer (DM) reaction scheme ($\frac{1}{2}A_2 + B \rightarrow AB$) as proposed by Ziff *et al* [1]. This model exhibits two irreversible phase transitions (IPTs) from a stationary regime with AB production to surface saturated states with A and B species [1, 3-5, 10-13, 15-21], respectively. The interesting critical behaviour of the DM model has been investigated by means of various techniques and using different kinds of substrata [4, 16-19]. Variants of the originally proposed DM model which accounts for variable reaction and adsorption rates [15], reactant's diffusion [11, 20] and desorption [21], etc, also exhibit interesting dynamic behaviour.

0305-4470/92/092557+12$04.50

In this work three models for the dimer-dimer (DD) surface reaction scheme of the type $\frac{1}{2}A_2 + B_2 \rightarrow B_2A$ are proposed and studied by means of Monte Carlo simulations and finite-size arguments. The models involve the formation of intermediate AB species on the surface, since they are inspired in the catalytic oxidation of hydrogen, i.e. $A_2 \equiv O_2$, $B_2 \equiv H_2$, $B_2A \equiv H_2O$ and $AB \equiv OH$. Likewise both the MM and the DM models, the studied models for the DD process, also exhibit IPTs. So, the critical points and the critical exponents of the relevant properties are determined. Since major interest in the study of particular models arises from the lack of a general theory to describe the observed rich variety of irreversible critical phenomena, it is expected that the occurrence of IPTs in the proposed DD models would stimulate further work in that direction.

2. The dimer–dimer surface reaction models and the simulation method

The model reaction proceeds according to the Langmuir-Hinshelwood (LH) reaction mechanism, i.e. both reactants have to be adsorbed on the catalyst surface; so

$$A_2(g) + 2(*) \rightarrow 2A(a) \tag{1a}$$

$$B_2(g) + 2(*) \underset{k_2}{\overset{k_1}{\rightleftharpoons}} 2B(a) \qquad (k_1 = \infty) \tag{1b}$$

$$A(a) + B(a) \rightarrow AB(a) + (*) \tag{1c}$$

$$AB(a) + B(a) \rightarrow B_2A(g) + 2(*) \tag{1d}$$

where $(*)$, (a), and (g) correspond to a vacant site of the surface, the adsorbed and gas phase, respectively, and k_1 and k_2 are the rate constants for B_2 adsorption and desorption, respectively.

Likewise for both the MM and DM models, the proposed mechanism for the DD process (equations $1a$–d) is not intended to represent that of any actual catalytic reaction, but to simulate a generic bimolecular LH reaction. Nevertheless, one has to recognize that the DM and DD models are inspired by the catalytic oxidation of carbon monoxide and hydrogen, respectively. The former has been, since Faraday in 1844 [22], extensively studied (for reviews up to 1980–81 see [23] and [24], and for more recent results see [25–27] and references therein).

In this work, three variants of the proposed mechanism are studied and they have been classified as follows: M1 $\equiv k_2 = 0$, i.e. the recombinative desorption of B_2 is not considered and surface diffusion of the adsorbed species is neglected; M2 $\equiv$ like M1 but assuming $B(a)$ diffusion; and M3 $\equiv$ like M2 but with $k_2 = \infty$, i.e. including B_2 desorption which may occur after recombination of two $B(a)$ species. Both diffusion of $B(a)$ species and desorption of B_2 dimers are assumed because H and H_2 are more mobile and desorb at lower temperature than O and O_2, respectively [25–27]. On the other hand it is assumed that the step which led to the formation of $AB(a)$ species (hydroxyl groups), equation $(1c)$, produces a vacant site on the surface based on the fact that OH groups are adsorbed through the O atom with the H one pointing away from the surface [24, 28]. Accumulation of the product (B_2A) on the surface can be neglected according to experimental results showing that water desorbs immediately after formation [25–27]. On the other hand, the recombination of $AB(a)$ species, which may play a role in the oxidation of hydrogen at low temperature [26, 27], will be studied in a forthcoming work [29]. The assumption that both A_2 and B_2 dimers can desorb simultaneously has not been considered because it prevents the occurrence of

truly saturated states with the reactants and consequently the existence of IPTs. Relevant data for the understanding of the models such as the rate of B_2A production (R), the surface coverage with $A(a)$, $B(a)$ and $AB(a)$ species (ϑ_A, ϑ_B and ϑ_{AB}, respectively) are studied as a function of the partial pressure of B_2 in the gas phase, namely p_{B_2}.

Simulations are performed in the square lattice of size L ($L \leqslant 600$) assuming periodic boundary conditions. The algorithm for the Monte Carlo simulation of the DD model, variant M1, can be summarized as follows: (i) A surface site is selected at random and if that site is occupied the trial ends; otherwise a B_2 (A_2) molecule is selected at random with probability p_{B_2} ($1-p_{B_2}$), respectively. (ii) Since in both cases one has to adsorb a dimer, a nearest-neighbour (NN) site is also selected at random. If that site is already occupied the trial ends because there is no place for dimer adsorption. Otherwise the dimer is adsorbed. (iii) After a successful adsorption of a dimer one has to investigate their six NN sites on the square lattice in order to check for the presence of $A(a)$ and $AB(a)$ species in the case of B_2 adsorption, and for $B(a)$ species in the case of A_2 adsorption. $A(a)$–$B(a)$ and $B(a)$–$AB(a)$ species occupying NN sites led to the formation of $AB(a)$ and $B_2A(g)$ and the corresponding number of vacant sites, respectively, according to the reaction scheme (1). AB species are formed on the site occupied by $A(a)$ while the site corresponding to $B(a)$ is vacated. When more than one NN of type $B(a)$ are found around a newly-adsorbed species of type A, one of them is selected at random in order to form an $AB(a)$ species, but this intermediate immediately reacts with one (randomly selected) of the remaining $B(a)$ to form $B_2A(g)$. Note that random selection of the $B(a)$ species is only relevant when the number of NNs is three. On the other hand, for a newly-adsorbed B species, there could be both $A(a)$ and $AB(a)$ NNs. If all NNs are of the same kind the reaction is decided at random. Otherwise, if one has NNs of different type, the formation of the product $B_2A(g)$ take precedence over the formation of the intermediate $AB(a)$.

Since model M2 includes $B(a)$ diffusion, one has to modify step (i). In fact, if the site selected at random is empty or occupied by $A(a)$ or $AB(a)$ species the algorithm proceeds as in the case M1. Otherwise, if the selected site (say site 1) is occupied by a $B(a)$ species a NN site (say site 2) is selected at random. If site 2 is occupied the trial ends, otherwise $B(a)$ is allowed to diffuse to site 2 while site 1 is vacated. So, simulations employ a fixed (unit) diffusion rate. After a successful diffusion event one has to investigate the three NN sites of site 2 (notice that site 1 can be excluded) in order to check for the presence of $A(a)$ and $AB(a)$ species as in step (iii) of M1.

Finally the algorithm for the variant M3 is based upon the M2 one but considering the desorption of B_2 dimers formed by two NN $B(a)$ species. This reaction followed by desorption left two vacant sites on the surface. Notice that $k_1 = \infty$ and $k_2 = \infty$ are used to symbolize that dimer adsorption on two NN empty sites and the recombination of $B(a)$ monomers adsorbed on two NN sites occur with probability one, respectively. Consequently, every B_2 which does not react on adsorption is desorbed.

The Monte Carlo time unit (t) is defined such that each site of the lattice may be visited once, on average. Simulations are performed until $t = 10^4$–10^5 and averages are taken after a suitable interval of time has elapsed (usually $t = 5 \times 10^3$) in order to avoid correlations with the transient period of the reaction. The time required for the system for relaxation depends on the proximity to the critical points; therefore it can be determined when stabilization of the monitored quantities, namely R, ϑ_A, ϑ_{AB} and ϑ_B, is observed. The simulations are performed in a multi-transputer system of five parallel T800 processors, hosted by a PC. The algorithms are written in OCCAM 2 [30], including the random number generator [31].

3. Results and discussion

Figure 1 shows the dependence of the surface coverage with $A(a)$, $B(a)$ and $AB(a)$ species (ϑ_A, ϑ_B, ϑ_{AB}, respectively) on the partial pressure of B_2 in the gas phase (p_{B_2}) for model M1. In this case one observed the occurrence of an IPT at the critical value of p_{B_2} given by $p_{1B_2}=\frac{2}{3}$. Runs performed using $p_{B_2}=0.6665$ and $p_{B_2}=0.6668$ led invariably to surface saturation, strongly suggesting that the critical point should be exactly $p_{1B_2}=\frac{2}{3}$. This statement is further supported by the stoichiometry of the reaction, as discussed below. Additionally, solving the mean field rate equations of the DD reaction process we have shown [32] for both models M1 and M2 the existence of a single critical point at $p_{1B_2}=\frac{2}{3}$.

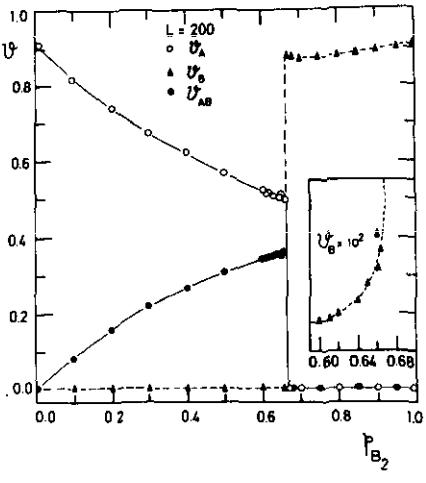

Figure 1. Plots of surface reactant coverages versus p_{B_2} for the model M1. The inset shows the dependence of ϑ_B on p_{B_2} just below the critical point $p_{1B_2}=\frac{2}{3}$. Data points are averages taken over 100 samples, and in most cases the error bars are smaller than the size of the point itself. More details in the text.

Dramatic changes occurring in the surface configuration of the adsorbed species in the neighbourhood of p_{1B_2} are shown in figure 2. It is found that for $p_{B_2}>p_{1B_2}$ the surface becomes saturated (poisoned) by $B(a)$ species and the production of B_2A always stops after a short transient period (figure 2(a)). Likewise, for $p_{B_2}\ll p_{1B_2}$ the surface is saturated by both $A(a)$ and $AB(a)$ species. Close to p_{1B_2} (but $p_{B_2}<p_{1B_2}$) the surface is also saturated, but now for $A(a)$, $AB(a)$ and a minority of $B(a)$ species, as is shown in the inset of figure 1 (see also figure 2(b)). The occurrence of small, but measurable, values of ϑ_B slightly below p_{1B_2} is due to the formation on the surface of small clusters (monomers in the particular example shown in figure 2(b)) of $B(a)$ particles surrounded by special configurations of empty sites which do not allow further adsorption of dimers requiring a pair of NN vacant sites. Notice that for $p_{B_2}\to 0$ and $p_{B_2}\to 1$ both ϑ_A and ϑ_B approach $\vartheta_A\simeq\vartheta_B\simeq 0.907$, which corresponds to the average occupancy probability of the random dimer adsorption problem [33, 34]. On the other hand for $p_{B_2}<p_{1B_2}$ ($p_{B_2}>p_{1B_2}$) one also has that $\vartheta_A+\vartheta_{AB}\simeq 0.9$ ($\vartheta_B\simeq 0.9$), respectively. So, at the saturated states there is always a certain fraction of vacant sites, but the reaction stops because there is no available place for dimer adsorption. These vacant

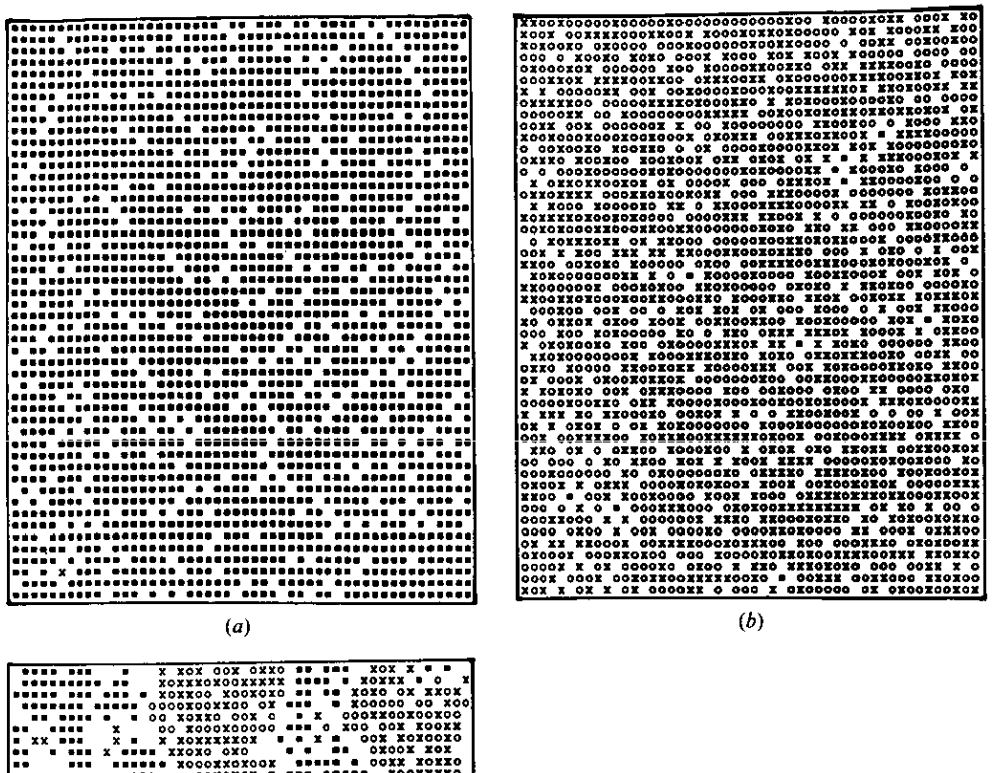

(*a*) (*b*) (*c*)

Figure 2. Typical snapshot configurations of the reactants on the surface characteristic of the model M1. Sample size $L = 50$, $\circ \equiv A(a)$, $\blacksquare \equiv B(a)$ and $\times \equiv AB(a)$, empty sites are left in white. (*a*) Saturated surface with $B(a)$ ($\vartheta_B \simeq 0.9$) after $t \simeq 10^3$ for $p_{B_2} = 0.68$, i.e. slightly above p_{1B_2}. (*b*) Saturated surface with $A(a)$ ($\vartheta_A \simeq 0.51$), $AB(a)$ $\vartheta_{AB} \simeq 0.35$ and few $B(a)$ monomers ($\vartheta_B \simeq 4 \times 10^{-3}$) after $t \simeq 10^3$ for $p_{B_2} = 0.65$, i.e. slightly below p_{1B_2}. (*c*) Configuration obtained during the stationary regime just at $p_{1B_2} = \frac{2}{3}$ for $t = 3 \times 10^3$, $\vartheta_A \simeq 0.13$, $\vartheta_B \simeq 0.45$ and $\vartheta_{AB} \simeq 0.13$.

sites can easily be distinguished in the typical configurations shown in both figures 2(*a*) and 2(*b*).

Finally, at the critical point $p_{1B_2} = \frac{2}{3}$ the production of B_2A remains almost stationary and the reaction seems to proceed indefinitely. Notice that this statement would be correct only in the limit $L \to \infty$ because coverage fluctuations occurring in finite systems would cause surface saturation at finite times. A typical snapshot of the surface configuration during the stationary regime with B_2A production just at p_{1B_2} is shown in figure 2(*c*). In this case one observes the growth of rather big islands and also some

small clusters formed on one side by $B(a)$ species and on the other one by a 'binary compound' of $A(a)$ and $AB(a)$ species. As can be observed in figure 2(c), vacant sites at the inner part of the islands are in most cases 'single sites'. Since dimer adsorption on these kind of sites is not possible, one concludes that the inner part of the islands does not contribute significantly to the production of B_2A, and consequently most reaction events should occur at the perimeter of the islands. In fact, islands have to be surrounded by empty sites and, in particular, reaction events occurring on these sites are responsible for the shape and size fluctuations of the islands.

The occurrence of a critical point at $p_{1B_2}=\frac{2}{3}$ is given by the stoichiometry of the DD reaction $B_2+\frac{1}{2}A_2\rightarrow B_2A$; likewise one has a critical point at $p_B=\frac{1}{2}$ for the MM reaction $A+B\rightarrow AB$ [2, 4, 6, 13, 14].

Results obtained with the M2 model are only slightly different from those already discussed. On the one hand, for $p_{B_2}>p_{1B_2}$ it is found that $\vartheta_B\rightarrow 1$ because, due to diffusion, the restrictions of the random dimer filling problem are somewhat relaxed. On the other hand, for p_{B_2} close to p_{1B_2} ($p_{B_2}<p_{1B_2}$), in contrast to the M1 model one has $\vartheta_B=0$ because $B(a)$ diffusion causes the formation of $AB(a)$ and $B_2A(g)$ species. Due to this effect, the coverages ϑ_A and ϑ_{AB} are slightly different from those of the model M1, but also in model M2 one has that $\vartheta_A+\vartheta_{AB}\simeq 0.9$ for $p_{B_2}<p_{1B_2}$.

Results corresponding to model M3 are shown in figure 3. Unlike in the previously discussed models M1 and M2, where the reaction proceeds only for a single value of p_{B_2}, namely the critical point p_{1B_2}, the recombinative reaction between two adjacent $B(a)$ species which led to B_2 desorption causes the occurrence of a reaction window. In fact, from figure 3 it follows that for $p_{B_2}\leq p_{1B_2}\simeq 0.7014$, the system is saturated by $A(a)$ and $AB(a)$ species (as in the cases of models M1 and M2), while at p_{1B_2} one observes an IPT to a state with B_2A production which remains stationary within the range $p_{1B_2}<p_{B_2}<1$. Some typical surface configurations of the reactants on the surface, within the stationary regime are shown in figure 4. They are quite different from that obtained for model M1 (figure 2(c)). In fact, figure 4(a) shows a snapshot of the surface for $p_{B_2}=0.79$, i.e. close to the value at which the rate of B_2A production is maximum (see figure 3). In this case the formation of small clusters of the binary compound $\{A(a)+AB(a)\}$ and few $B(a)$ monomers can be observed. The total surface

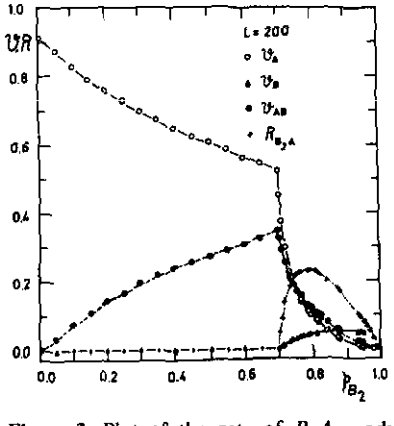

Figure 3. Plot of the rate of B_2A production (R) and the surface coverages with the reactants versus p_{B_2} for the model M3. Data points are averages taken over 100 (10) samples for $p_{B_2}<p_{1B_2}$ ($p_{B_2}>p_{1B_2}$), respectively. In most cases the error bars are smaller than the size of the point itself. More details in the text.

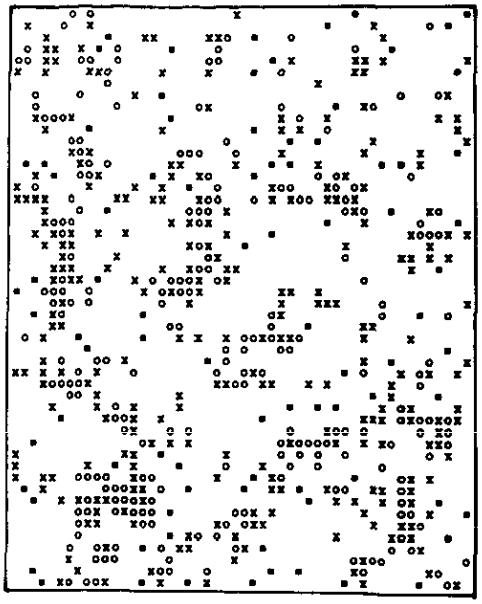

(*a*)

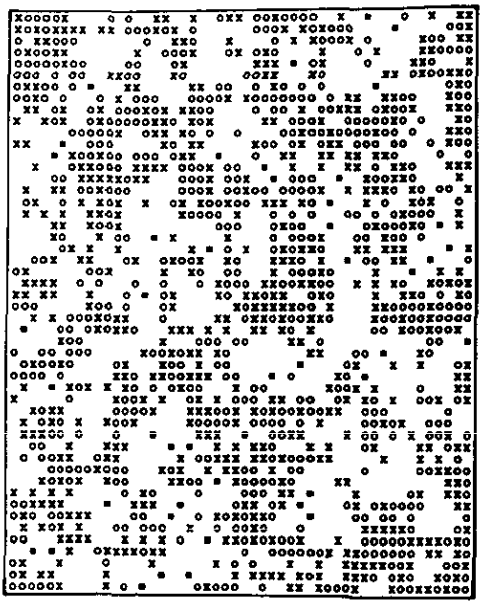

(*b*)

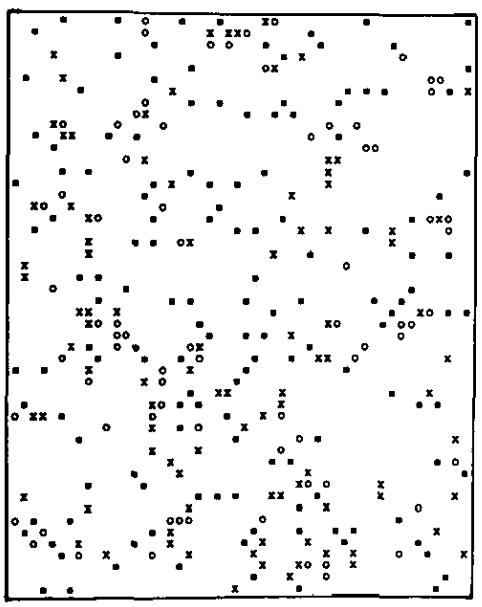

(*c*)

Figure 4. Typical snapshot configurations of the reactants on the surface characteristic of the model M3 during the stationary regime with B_2A production. Sample size $L = 50$ and $t = 3 \times 10^3$, $\bigcirc \equiv A(a)$, $\blacksquare \equiv B(a)$ and $\times \equiv AB(a)$, empty sites are left in white. (*a*) $p_{B_2} = 0.79$, i.e. close to the maximum of B_2A production, $\vartheta_A \simeq 0.10$, $\vartheta_B \simeq 0.035$ and $\vartheta_{AB} \simeq 0.11$. (*b*) $p_{B_2} = 0.725$, $\vartheta_A \simeq 0.27$, $\vartheta_B \simeq 0.02$ and $\vartheta_{AB} \simeq 0.24$. (*c*) $p_{B_2} = 0.90$, $\vartheta_A \simeq 0.03$, $\vartheta_B \simeq 0.06$ and $\vartheta_{AB} \simeq 0.04$.

coverage is $\vartheta_A + \vartheta_{AB} + \vartheta_B \simeq 0.24$, so most surface sites remain vacant. To the left of the B_2A production maximum, figure 4(*b*) for $p_{B_2} = 0.725$, nearly 50% of the surface is covered by islands and small clusters of the binary compound. Also, few $B(a)$ monomers are adsorbed. Slightly below and just at the critical point the surface configurations are quite similar to those of the model M1 obtained under equivalent conditions; see, for example, figure 2(*b*). It is interesting to note that at $p_{1B_2} \simeq 0.7014$ *the surface coverage* $\vartheta_A \simeq 0.55$ *is within the range of critical probabilities* (p_c) already determined for various percolation models given, for example by $0.47 \leqslant p_c \leqslant 0.66$

[35-39]; for reviews on the percolation theory see [39]. So, one may consider, among others, the following two possibilities: (i) Both components of the binary compound are well mixed preventing the formation of $A(a)$ percolating clusters; or (ii) $A(a)$ islands may span the whole lattice forming some sort of 'backbone' to which $AB(a)$ species (the minority) can attach. Since at p_{1B_2} percolating clusters of $A(a)$ species are not found, possibility (ii) has to be disregarded while (i) seems to be in qualitative agreement with the configuration shown in figure 4(b). To the right of the B_2A production maximum, figure 4(c) for $p_{B_2} \simeq 0.9$, only 10% of the surface is covered by small clusters (mostly monomers) of the reactants but in contrast to figures 4(a) and 4(b), $\vartheta_A < \vartheta_{AB} < \vartheta_B$ as expected from figure 3.

In order to further investigate the critical behaviour of model M3, notice that working with finite lattices one can only determine L-dependent 'critical points' [16, 17] (say $p_{cB_2}(L)$) as usually happens in the study of reversible phase transitions using the Monte Carlo method [40]. This statement is illustrated in figure 5 where the poisoning (saturation) probability (PP) is plotted against p_{B_2} for lattices of size $L = 65$ and $L = 100$. PPs are evaluated performing 10^2 Monte Carlo simulations with different samples up to a maximum time of $t = 10^4$. Under these conditions the 'critical points' $p_{cB_2}(L)$ are determined at the limit PP $\to 0$ and assuming error bars given by the interval between consecutive data points. Even for rather small lattices, like those used in the example of figure 5, this procedure is time consuming. This shortcoming is avoided when working with bigger lattices ($L > 100$, see figure 6) because one needs only to make a detailed scan of p_{B_2} values close to the limit PP $\to 0$.

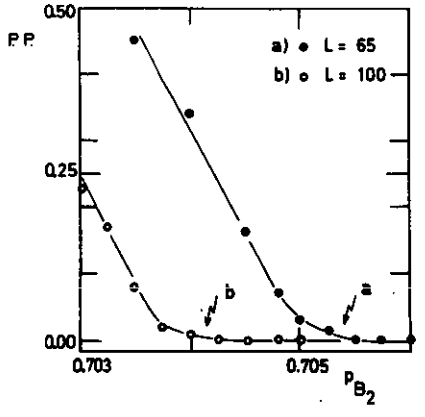

Figure 5. The poisoning probability (PP) with $A(a)$ and $AB(a)$ species as a function of p_{B_2} for samples of different size. The arrows show the L-dependent critical probabilities $p_{cB_2}(L)$. More details in the text.

Figure 6 shows a plot of $p_{cB_2}(L)$ versus L^{-1} and the obtained straight line allows us to determine $p_{1B_2}(L \to \infty) \simeq 0.7014$ using least-square regression and neglecting end-points for small lattices ($L \leq 50$). It should be noticed that the L-dependent 'critical probabilities' would also depend on the particular conditions assumed for their determination; for example performing a different number of Monte Carlo simulations or waiting for poisoning during a different period of time. Nevertheless it is expected that the $L \to \infty$ critical value p_{1B_2} may be independent of the employed method.

A precise determination of the critical point at which the IPT of the DD model M3 take place allow us to study its critical behaviour. In order to do this, power law

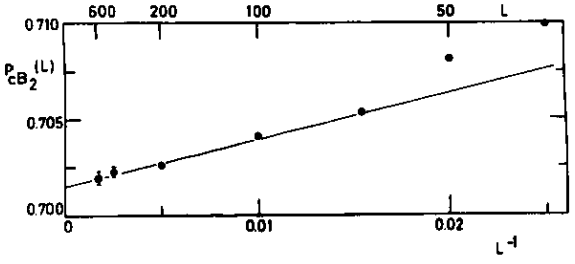

Figure 6. The L-dependent critical probabilities $p_{cB_2}(L)$ plotted against the inverse of the lattice size (L^{-1}). In most cases the error bars are the size of the point itself or smaller. The straight line is a least-squares fit of the data (neglecting end-points corresponding to smaller lattices ($L \leq 50$)) which intercepts the vertical axis at the $L \to \infty$ critical probability given by $p_{1B_2} \simeq 0.7014$. More details in the text.

dependence of the relevant quantities are proposed, so

$$R \propto (p_{B_2} - p_{1B_2})^{\beta_1} \qquad p_{B_2} > p_{1B_2} \tag{2}$$

and

$$\vartheta_B \propto (p_{B_2} - p_{1B_2})^{\beta_2} \qquad p_{B_2} > p_{1B_2} \tag{3}$$

where β_1 and β_2 are critical exponents. Note that both $R = 0$ and $\vartheta_B = 0$ when $p_{B_2} = p_{1B_2}$. The critical behaviour of ϑ_A and ϑ_{AB} is analysed simultaneously by assuming that for $L \to \infty$ one has $\vartheta_A + \vartheta_{AB} \simeq 0.907$ when $p_{B_2} = p_{1B_2}$; i.e. the best estimate of the random filling dimer problem [33, 34] which is also in excellent agreement with the Monte Carlo results of the present work, as has already been discussed. Therefore, the following power law dependence is assumed

$$\Delta\vartheta = (0.907 - \vartheta_A - \vartheta_{AB}) \propto (p_{B_2} - p_{1B_2})^{\beta_3} \qquad p_{B_2} > p_{1B_2} \tag{4}$$

where β_3 is also a critical exponent.

Figure 7 shows a log–log plot of R versus Δp ($\Delta p = p_{B_2} - p_{1B_2}$) obtained using samples of different size but taking in all cases $p_{B_2} > p_{cB_2}(L)$; i.e. when PP = 0, in order to avoid finite-size effects. For this reason the critical probability can only be closely approached ($\Delta p \simeq 2 \times 10^{-4}$) using large samples (see figure 7). The straight line with slope $\beta_1 = 1$ suggest that R increases linearly near the critical region.

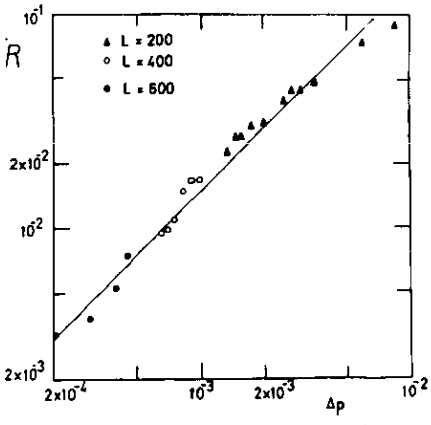

Figure 7. Log–log plot of R versus Δp (see equation (2)) for lattices of different size. The straight line with slope $\beta_1 = 1$ has been drawn for comparison.

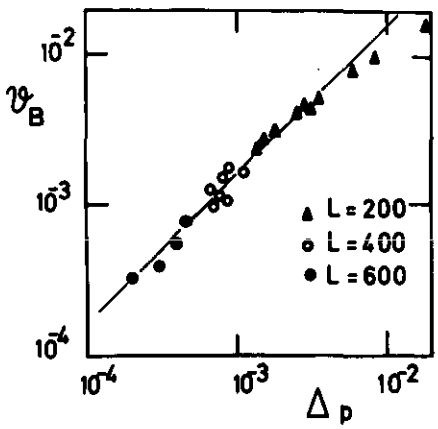

Figure 8. Log–log plot of ϑ_B versus Δp (see equation (3)) for lattices of different size. The straight line with slope $\beta_2 = 1$ has been drawn for comparison.

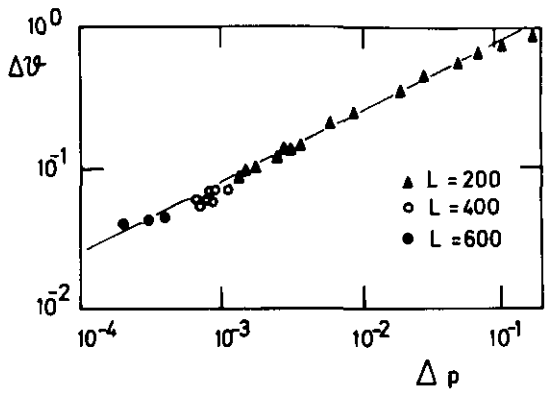

Figure 9. Log–log plot of $\Delta\vartheta$ versus Δp (see equation (4)) for lattices of different size. The straight line with slope $\beta_3 = \frac{1}{2}$ has been drawn for comparison.

In order to test the power law assumption of (3), figure 8 shows a log–log plot of ϑ_B versus Δp. In this case also, the obtained straight line with slope $\beta_2 = 1$ suggests linear growth of B-species coverage close to the critical point. Finally, a log–log plot of $\Delta\vartheta$ versus Δp (figure 9) also shows a straight line behaviour, but now with slope $\beta_3 = \frac{1}{2}$. Note that all exponents are approximated by exact fractions or integer numbers within an estimated error of ±5% or less. Summing up, the conjectured power law dependences (equations (2)–(4)) are found to hold in the region close to the critical point and the corresponding critical exponents can be evaluated.

4. Conclusions

The critical behaviour of three models for the DD ($\frac{1}{2}A_2 + B_2 \rightarrow B_2A$) surface reaction scheme is studied by means of Monte Carlo simulations on the square lattice. In absence of surface diffusion and desorption (model M1) a critical point at $p_{1B_2} = \frac{2}{3}$ is found such that, for $p_{B_2} > p_{1B_2}$ ($p_{B_2} < p_{1B_2}$), the surface becomes saturated by $B(a)$

species (a binary compound formed by $A(a)$ and $AB(a)$ species, respectively). The reaction has a stationary state with B_2A production only at p_{1B_2}. Incorporating the surface diffusion of $B(a)$ species (model M2) the critical point does not change, and only minor changes in the dependence of ϑ_A, ϑ_B and ϑ_{AB} on p_{B_2} are found when compared with results from M1. So, surface diffusion does not affect the overall critical behaviour of the studied DD scheme.

Assuming the desorption of B_2 dimers as a consequence of the recombinative reaction of $B(a)$ species (model M3), a richer and more interesting critical behaviour is observed. In fact, using a finite-size analysis a critical point is found at $p_{1B_2} \simeq 0.7014$ $(L \to \infty)$. For $p_{B_2} \leqslant p_{1B_2}$ the surface is saturated by $A(a)$ and $AB(a)$ species and for $p_{1B_2} < p_{B_2} < 1$ the system reaches a reactive stationary state with B_2A production. Close to the irreversible phase transition at p_{1B_2} the relevant quantities under study, namely R, ϑ_B and $(\vartheta_A + \vartheta_{AB})$ exhibit simple power law behaviour with critical exponents $\beta_1 = 1$, $\beta_2 = 1$ and $\beta_3 = \frac{1}{2}$, respectively.

The study of the rich variety of critical phenomena exhibited by these simple models, inspired in the catalytic oxidation of hydrogen, suggests that Monte Carlo simulations may have much to contribute to the understanding of heterogeneous catalysis. Also it is expected that the occurrence of IPTs in the DD surface reaction scheme, and particularly in model M3, will stimulate further effort in the development of a suitable theory for irreversible dynamic reactions. An extension of the DD model to account for the recombination reaction of $AB(a)$ species is in progress.

Acknowledgments

This work is financially supported by the Consejo Nacional de Investigaciones Científicas y Técnicas (CONICET) de la República Argentina. The author wishes to acknowledge the Alexander von Humboldt Foundation (Germany) for the provision of valuable equipment.

References

[1] Ziff R M, Gulari E and Barshad Y 1986 *Phys. Rev. Lett.* **56** 2553
[2] Ziff R M and Fichthron K 1986 *Phys. Rev.* B *(Rapid Commun.)* **34** 2038
[3] Dickman R 1986 *Phys. Rev.* A **34** 4246
[4] Meakin P and Scalapino D J 1987 *J. Chem. Phys.* **87** 731
[5] Chopard B and Droz M 1988 *J. Phys. A: Math. Gen.* **21** 205
[6] Sadiq A and Yaldram K 1988 *J. Phys. A: Math. Gen.* **21** L207
[7] Fichthron K, Gulari E and Ziff R M 1989 *Phys. Rev. Lett.* **63** 1527
[8] Fichthron K, Gulari E and Ziff R M 1989 *Chem. Ing. Sci.* **44** 1403
[9] Khan M A and Yaldram K 1989 *Surf. Sci.* **219** 445
[10] Yaldran K and Sadiq A 1989 *J. Phys. A: Math. Gen.* **22** 1925
[11] Fisher P and Titulaer U M 1989 *Surf. Sci.* **221** 409
[12] Browne D A and Kleban P 1989 *Phys. Rev.* A **40** 1615
[13] ben-Avraham D, Redner S, Considine D and Meakin P 1990 *J. Phys. A: Math. Gen.* **23** L613
[14] ben-Avraham D, Considine D, Meakin P, Redner S and Takayasu H 1990 *J. Phys. A: Math. Gen.* **23** 4297
[15] Considine D, Takayasu H and Redner S 1990 *J. Phys. A: Math. Gen.* **23** L1181
[16] Albano E V 1990 *J. Phys. A: Math. Gen.* **23** L545
[17] Albano E V 1990 *Phys. Rev.* B *(Rapid Commun.)* **42** 10818
[18] Albano E V 1990 *Surf. Sci.* **235** 351

[19] Albano E V 1991 *J. Chem. Phys.* **94** 1499
[20] Jensen I and Fogedby H C 1990 *Phys. Rev.* A **42** 1969
[21] Albano E V 1992 *Appl. Phys.* A in press
[22] Faraday M 1844 *Experimental Researches in Electricity* (London)
[23] Norton P R 1982 *Chemical Physics of Solid Surfaces and Heterogeneous Catalysis* vol 4, ed D A King and D P Wooddruff (Amsterdam: Elsevier) p 27
[24] Nieuwenhys B E 1983 *Surf. Sci.* **126** 307
[25] Helling B, Kasemo B, Ljungström S, Rosén A and Wahnström T 1987 *Surf. Sci.* **189/90** 851
[26] Ljungström S, Kasemo B, Rosén A, Wahnström T and Fridell E 1989 *Surf. Sci.* **216** 63
[27] Wahnström T, Fridell E, Ljungström S, Helling B, Kasemo B and Rosén A 1989 *Surf. Sci.* **223** L905
[28] Yang H and Whitten J L 1989 *Surf. Sci.* **223** 131
[29] Albano E V 1991 *J. Stat. Phys.* submitted
[30] Jones G and Goldsmith M 1988 *Programming in OCCAM 2* ed C A R Hoare (International Series in Computer Science) (London: Prentice-Hall)
[31] Paul W, Heermann D W and Desai R C 1989 *J. Comp. Phys.* **82** 489
[32] Maltz A and Albano E V 1992 in preparation
[33] Evans J W, Burgess D R and Hoffman D K 1983 *J. Chem. Phys.* **79** 5011
[34] Evans J W and Nord R S 1985 *Phys. Rev.* B **31** 1759
[35] Mártin H O, Albano E V and Maltz A 1987 *J. Phys. A: Math. Gen.* **20** 1531
[36] Albano E V and Mártin H O 1987 *Thin Solid Films* **151** 121
[37] Mártin H O and Albano E V 1988 *Z. Phys.* B **70** 213
[38] Anderson S R and Family F 1988 *Phys. Rev.* A **38** 4198
[39] Stauffer D 1985 *Introduction to the Percolation Theory* (London: Taylor and Francis)
[40] Binder K ed 1979 *Monte Carlo Methods in Statistical Physics* (Berlin: Springer)